Photoinduced Electron Transfer and Adduct Formation between C_{60}/C_{70} and Optically Active 1,1′-Binaphthyl-2,2′-diamine

Maged El-Kemary,[†] Mamoru Fujitstuka,[‡] and Osamu Ito*[,‡]

Institute for Chemical Reaction Science, Tohoku University, Katahira, Aoba-ku, Sendai 980-8577, Japan, and Department of Chemistry, Faculty of Education, Tanta University, Kafr El-Sheikh, Egypt

Received: June 30, 1998; In Final Form: December 31, 1998

Photoinduced electron transfer and adduct formation between C_{60}/C_{70} and 1,1′-binaphthyl-2,2′-diamine (BNA) have been studied by nanosecond laser flash photolysis and steady-state photolysis as well as circular dichroism measurements. Quantum yields (Φ_{et}^{T}) and rate constants of electron transfer from BNA to the excited triplet state of C_{60}/C_{70} have been determined by observing the transient absorption bands in the near-IR region where the triplet states and anion radicals of fullerenes appear. Compared with the planar naphthylamine moiety, Φ_{et}^{T} values of perpendicular bichromophoric BNA are low because of hindrance of approach to round fullerenes. The formation of an optically active adduct between C_{60} and BNA in a polar solvent was observed upon excitation with light at $\lambda > 330$ nm where both C_{60} and BNA are light-absorbing. The reaction mechanism for the optically active adduct formation can be explained as a result of the addition reaction of the N-centered radical formed by deprotonation of $BNA^{\bullet+}$, which is produced by direct photoejection.

Introduction

Photoinduced electron transfer is an important subject, since it provides a good model system to investigate the dynamic aspects of charge separation and charge recombination systems. Time-resolved measurements will lead to a better understanding of the general feature of electron-transfer mechanisms. Photoexcitation of fullerenes such as C_{60} and C_{70} increases their high electron-acceptor abilities in the presence of electron donors such as aliphatic and aromatic amines.[1−8] So far, the aromatic amines are usually restricted to planar ones. In the present study, we employed 1,1′-binaphthyl-2,2′-diamine (BNA), since BNA has a structure with two perpendicular naphthylamine moieties; thus, it is interesting to examine such sterical effect on the electron-transfer efficiency.

BNA has molecular asymmetry, existing as optically active isomers; photochemical reactions between optically active BNA and C_{60}/C_{70} would be expected to be selectively followed by the circular dichroism (CD), which might be induced with the C_{60}/C_{70} chromophore only when optically active adducts BNA−C_{60}/C_{70} are produced. Although higher fullerenes such as C_{76} have been reported to be chiral,[9] it is necessary to introduce a chiral center to fullerenes such as C_{60} in order to obtain optically active fullerene derivatives.[10−14] Fullerene derivatives with chiral centers in the substituents were reported to exhibit CD spectra.[10−14]

In the present report, we measured the transient absorption spectra for C_{60}/C_{70} and BNA in the vis/NIR regions together with the steady-state CD spectra. The electron-transfer efficiencies to the triplet states of C_{60}/C_{70} ($^3C_{60}^*/^3C_{70}^*$) from BNA are significantly different from those of planar *N*-phenyl-β-naphthylamine (PNA), suggesting some kind of steric effects. Formation of optically active adduct between C_{60} and BNA is restricted to some specific experimental conditions. Transient absorption measurements in addition to CD measurements allow us to examine the mechanism of the formation of optically active products.

Experimental Section

C_{60} and C_{70} were obtained in a purity of 99.9% from Texas Fullerenes Corp. Commercially available optically active 1,1′-binaphthyl-2,2′-diamine (BNA) (Aldrich Co. Ltd.) was used as received. *N*-Phenyl-β-naphthylamine (PNA) was recrystallized from ethanol. Benzonitrile and benzene used as solvents were of HPLC and spectrophotometric grade, respectively. The solution of C_{60} (or C_{70}) and BNA (or PNA) was deaerated by Ar bubbling for 15 min before measurements.

The solution of C_{60}/C_{70} and/or BNA/PNA was selectively excited by either 532 or 355 nm light from a Nd:YAG laser (Quanta-Ray; 6 ns fwhm) with 7 mJ power. For the transient absorption spectra in the visible region, an Si PIN photodiode (Hamamatsu) was used as a detector to monitor the transmitted light from a pulsed Xe lamp (150 W) passing through a rectangular quartz reaction cell (1 cm) and monochromator.[15] In the NIR region, a Ge avalanche photodiode (Hamamatsu) was employed as a detector. Steady-state photolysis was carried out with a Xe−Hg lamp (150 W); the wavelength region of light was selected by cutoff filters. The steady-state UV/vis absorption spectra were measured with a JASCO/V-570 spectrophotometer. The absorption spectra of the cation radicals of amines were measured by γ-radiolysis in butyl chloride at 77 K. The circular dichroism (CD) spectra were measured on a JASCO/I-0015 spectropolarimeter. All experiments were carried out at 23 °C.

Results and Discussion

Steady-State UV/Visible Spectra. Steady-state UV/vis spectra of C_{60}, BNA, and PNA in benzonitrile were recorded between 350 and 700 nm as shown in Figure 1. On the addition of BNA or PNA, the absorption intensity of C_{60} in the visible region

[†] Tanta University.
[‡] Tohoku University.

10.1021/jp9828383 CCC: $18.00
Published on Web 02/20/1999

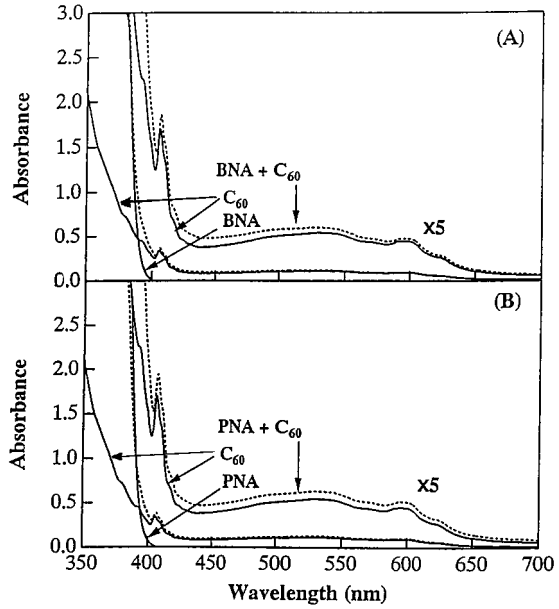

Figure 1. Steady-state absorption in the UV/vis region: (A) C_{60} (0.1 mM), BNA (3 mM), and their mixtures in benzonitrile; (B) C_{60} (0.1 mM), PNA (6 mM), and their mixtures in benzonitrile.

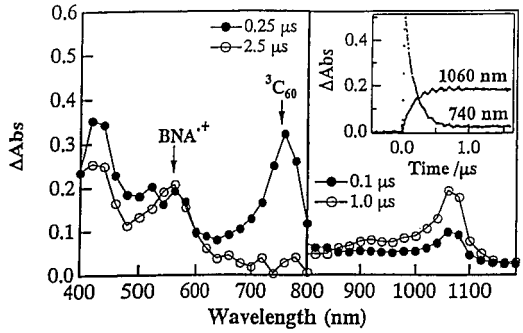

Figure 2. Transient absorption spectra obtained by 532 nm laser photolysis of C_{60} (0.1 mM) in the presence of BNA (3 mM) in Ar-saturated benzonitrile. Detector is Si PIN (800−600 nm) and Ge APD (800−1200 nm). Insert shows time profiles.

increases, accompanied by subtle changes in position and shape of the absorption band. Compared with BNA/C_{60}, a more significant increase in the absorption for PNA/C_{60} is confirmed under the condition where PNA concentration is twice that of bichromophoric BNA. Since such spectral changes generally imply the formation of a weak charge-transfer (CT) complex, it is presumed that the CT interaction of the planar PNA is slightly stronger than the perpendicular BNA. Similar behavior was observed in the case of C_{70}. Since both BNA and PNA have appreciable absorption in wavelength region shorter than 400 nm, C_{60} and C_{70} can be selectively excited by 532 nm laser light, while both fullerenes and BNA (or PNA) can be excited by 355 nm light.

Photoinduced Electron Transfer. Figure 2 shows the transient absorption spectra in the vis/NIR region obtained by the laser flash photolysis of C_{60} with 532 nm light in the presence of BNA (3 mM) in deaerated benzonitrile. The transient absorption band at 740 nm is attributed to the triplet−triplet (T−T) absorption of C_{60} ($^3C_{60}$*).[16,17] With the decay of $^3C_{60}$*, a new absorption band appears at 1060 nm with a shoulder at 900 nm, which is assigned to the absorption of $C_{60}^{\bullet-}$.[18−21] In the visible region, the transient bands that appeared immediately after the laser pulse are attributed to $^3C_{60}$*, while

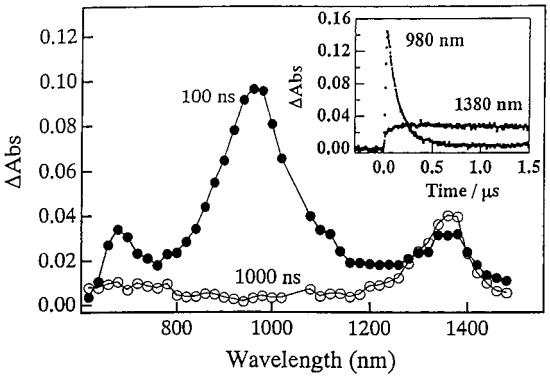

Figure 3. Transient absorption spectra obtained by 532 nm laser photolysis of C_{70} (0.1 mM) in the presence of BNA (3 mM) in Ar-saturated benzonitrile. Insert shows time profiles.

the absorption band remaining at 520 nm can be assigned to the BNA cation radical ($BNA^{\bullet+}$).

The observed time profiles of the absorption bands are shown in the inset of Figure 2. The decay of $^3C_{60}$* at 740 nm, which did not show appreciable decay over a few microseconds without BNA, was accelerated in the presence of BNA (3 mM). With the decay of $^3C_{60}$*, the absorption intensity of $C_{60}^{\bullet-}$ at 1060 nm increases, reaching a maximum at about 0.7−1.0 μs. The decay of $^3C_{60}$* and the appearance of $C_{60}^{\bullet-}$ are proof of the electron-transfer process in which $C_{60}^{\bullet-}$ is produced via $^3C_{60}$* by accepting an electron from BNA. By use of the molar absorption coefficient (ϵ_T) of $^3C_{60}$* at 740 nm (16 000 M^{-1} cm^{-1}),[22] the initial maximum concentration of $^3C_{60}$* ($[^3C_{60}^*]_{max}$) produced by a laser pulse is calculated. The maximum concentration of $C_{60}^{\bullet-}$ ($[C_{60}^{\bullet-}]_{max}$) at 1 μs was also determined using the reported molar extinction coefficients (ϵ_A) of $C_{60}^{\bullet-}$ in benzonitrile (12 000 M^{-1} cm^{-1} at 1070 nm).[21,22]

With 532 nm laser excitation of C_{70} in benzonitrile (Figure 3), the main absorption at 980 nm and the weak one at 680 nm due to $^3C_{70}$* were quenched by the addition of BNA,[23−27] concomitantly with appearance of the absorption band of $C_{70}^{\bullet-}$ at 1380 nm.[18−21,28−30] As shown in the inserted time profile of Figure 3, the absorption intensity at 1380 nm begins to rise immediately after the laser pulse followed by a slow rise, which corresponds to the decay of $^3C_{70}$*. The initial fast rise of 1380 nm may be ascribed to the absorption tail of $^3C_{70}$*. $[^3C_{70}^*]_{max}$ and $[C_{70}^{\bullet-}]_{max}$ were calculated using the reported ϵ_T value (6500 M^{-1} cm^{-1} at 980 nm)[21] and ϵ_A value (4000 M^{-1} cm^{-1} at 1370 nm),[28] respectively.

The contribution of the singlet states of C_{60}/C_{70} ($^1C_{60}$*/$^1C_{70}$*) to $C_{60}^{\bullet-}/C_{70}^{\bullet-}$ formation was not necessary to take into consideration because the rises of $C_{60}^{\bullet-}$ are slow as shown in the insert of Figure 2.

The effect of PNA concentration on the time profiles for the decay of $^3C_{60}$* are shown in Figure 4A. It is apparent that the decay rates of $^3C_{60}$* increase with [PNA]. Each decay curve of $^3C_{60}$* in the presence of PNA was fitted with a single exponential, while weak nondecaying absorbance may be attributed to $PNA^{\bullet+}$,[31] which did not affect the kinetic analysis. The second-order rate constant (k_q) was obtained from the linear dependence of k_{1st} on [PNA] as shown in the insert of Figure 4A. The obtained k_q values are listed in Table 1.

The rates of $C_{60}^{\bullet-}$ rise increase with [PNA] in benzonitrile as shown in Figure 4B. Each rise curve was fitted with a single exponential, yielding k_{1st} without taking the decay of $C_{60}^{\bullet-}$ into consideration. The second-order rate constant k_A (where subscript A represents $C_{60}^{\bullet-}$ or $C_{70}^{\bullet-}$) was obtained by plotting k_{1st} vs [PNA] (Figure 4B). The obtained k_A values are in good

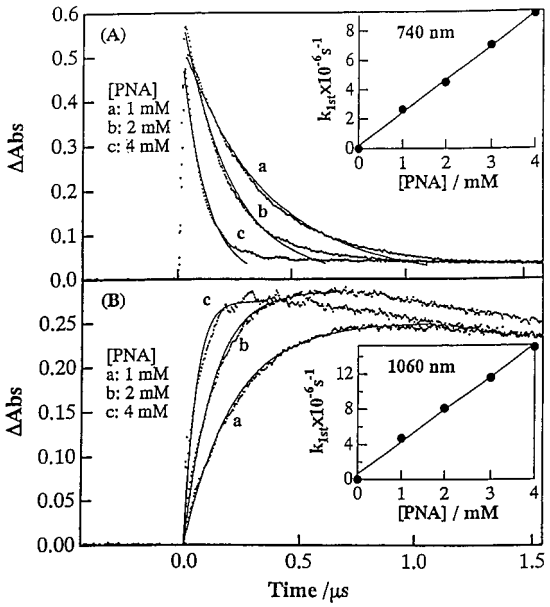

Figure 4. (A) Decay profiles of $^3C_{60}$* at 740 nm with changing [PNA]. Insert shows pseudo-first-order plot. (B) Rise profiles of $C_{60}^{\bullet-}$ at 1060 nm with changing [PNA]. Insert shows pseudo-first-order plot.

TABLE 1: Rate Constants and Quantum Yields for Electron Transfer

fullerene/ amine	solvent[a]	k_q/ $M^{-1}s^{-1}$ [b]	Φ_{et}^T	k_{et}/ $M^{-1}s^{-1}$ [b]	k_{et}^{NA}/ $M^{-1}s^{-1}$ [c]
C_{60}/PNA	BN	2.2×10^9	0.82	1.8×10^9	1.8×10^9
C_{60}/BNA	BN	1.8×10^9	0.49	8.8×10^8	4.4×10^8
C_{60}/BNA	BN/BZ	3.2×10^9	0.43	1.4×10^9	7.0×10^8
C_{70}/PNA	BN	1.4×10^9	0.63	8.8×10^8	8.8×10^8
C_{70}/BNA	BN	2.2×10^9	0.40	8.8×10^8	4.4×10^8
C_{70}/BNA	BN/BZ	2.5×10^9	0.33	8.3×10^8	4.2×10^8

[a] BN, benzonitrile; BZ, benzene; BN/BZ = 1:1 mixture. [b] $k_{et} = k_q \times \Phi_{et}^T$. [c] k_{et}^{NA} refers to electron-transfer rate constant per 1 NA moiety ($=k_{et}/2$).

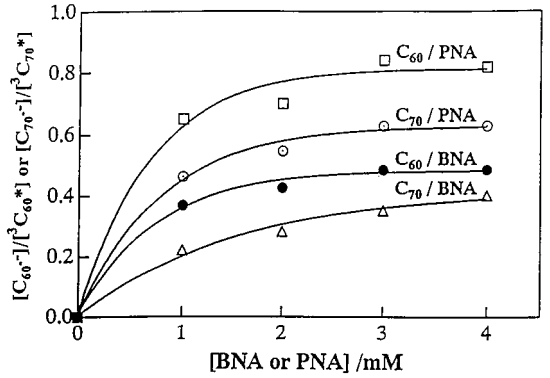

Figure 5. Dependence of $[C_{60}^{\bullet-}]/[^3C_{60}*]$ and $[C_{70}^{\bullet-}]/[^3C_{70}*]$ on [BNA] and [PNA] in benzonitrile.

agreement with the corresponding k_q values within the experimental errors.

The efficiency of electron transfer via $^3C_{60}$* or $^3C_{70}$* can be estimated by the quantity $[C_{60}^{\bullet-}]/[^3C_{60}*]$ (or $[C_{70}^{\bullet-}]/[^3C_{70}*]$) as evaluated by the maximal and initial absorbances and reported ϵ_A and ϵ_T. In Figure 5, $[C_{60}^{\bullet-}]/[^3C_{60}*]$ and $[C_{70}^{\bullet-}]/[^3C_{70}*]$ are plotted against [BNA] or [PNA] in benzonitrile. The efficiencies increase, reaching a plateau, from which the quantum yield (Φ_{et}^T) for electron transfer to the triplet state was estimated. For both C_{60} and C_{70}, the Φ_{et}^T values of BNA are lower than those of PNA by a factor of ca. 0.5, which is particularly interesting in regard to molecular structure of donors. A possible explanation of this observation is that the approach of perpendicular BNA to round fullerenes is hindered, while planar PNA easily makes contact with fullerene molecules. This reflects the slightly strong ground-state CT interaction of fullerenes/PNA compared with that of fullerenes/BNA (Figure 1). As for the difference in the acceptor abilities between C_{60} and C_{70}, the Φ_{et}^T values of C_{60} are faintly higher than those of C_{70} for both PNA and BNA, suggesting that C_{60} is a slightly stronger acceptor than C_{70}.

The rate constant for electron transfer (k_{et}) can be evaluated from the relation $k_{et} = \Phi_{et}^T \times k_q$.[32] The obtained k_{et} values (Table 1) are smaller than the diffusion-controlled limit ($k_{diff} = 5.6 \times 10^9$ M^{-1} s^{-1} in benzonitrile) by a factor of about 0.2. Such small k_{et} values are in accord with the reported tendency for electron transfer to fullerenes.[17b,33] It is clear that the values of k_{et} per one naphthylamine moiety (NA) for BNA, which refers to k_{et}^{NA} in Table 1, are smaller than those for PNA. This gives further support to steric hindrance of an approach of perpendicular BNA to round fullerenes.

Solvent Effect on Photoinduced Electron Transfer. In a less polar solvent [1:1 mixture of benzonitrile to benzene, BN/BZ (1:1)], the transient absorption spectra for C_{60}/BNA or C_{70}/BNA displayed much the same features as in benzonitrile. The main difference includes the low intensity of $C_{60}^{\bullet-}/C_{70}^{\bullet-}$ relative to that of $^3C_{60}*/^3C_{70}*$, indicating slightly lower Φ_{et}^T than those in benzonitrile (Table 1). On the other hand, a faster decay rate of $^3C_{60}*/^3C_{70}*$ and the faster rise of $C_{60}^{\bullet-}/C_{70}^{\bullet-}$ in the less polar solvent yielded larger k_q and k_A values; the k_{et} values obtained by multiplying Φ_{et}^T are listed in Table 1. In the case of C_{70}, the k_{et} value in a less polar solvent is almost the same as that in a polar solvent, which can be explained by the segregation effect of mixed solvents; i.e., polar solvents predominantly solvate the ion radicals. For C_{60}, the k_{et} value in BN/BZ (1:1) is larger than that in benzonitrile; this finding is difficult to interpret.

In nonpolar solvents, neither the rise of $C_{60}^{\bullet-}$ nor the decay of $^3C_{60}$* was observed on the addition of BNA (or PNA), indicating the absence of any deactivation processes of $^3C_{60}$*. In the case of C_{70}, the decay rate of $^3C_{70}$* was slightly increased on the addition of BNA (or PNA), although $C_{70}^{\bullet-}$ was not observed in the nonpolar solvent. This is probably attributed to slow deactivation processes such as collisional quenching, which takes place without electron transfer.

Back Electron Transfer. Figure 6 shows the time profiles of $C_{60}^{\bullet-}$ and $C_{70}^{\bullet-}$ on the long-time scale. It is clear that the anion radicals begin to decay slowly after reaching each maxima. This can be attributed mainly to the back electron transfer from $C_{60}^{\bullet-}/C_{70}^{\bullet-}$ to $BNA^{\bullet+}/PNA^{\bullet+}$ because extra reactions such as adduct formation were not observed in the steady-state absorption spectra after irradiation of C_{60}/C_{70} with 532 nm light in the presence of BNA/PNA. The decay time profiles obey second-order kinetics. From the slope of the second-order plot in the insert of Figure 6, k_{bet}/ϵ_A was evaluated. The back electron-transfer rate constants (k_{bet}) were evaluated by substituting the reported ϵ_A values as listed in Table 2. It should be noted that the k_{bet} values for $C_{60}^{\bullet-}/BNA^{\bullet+}$ and $C_{70}^{\bullet-}/BNA^{\bullet+}$ decrease with increasing solvent polarity, owing to the strong solvation of the ion radicals in more polar solvents. In benzonitrile, the values of k_{bet} are close to the diffusion-controlled limit except for the C_{70}/BNA system. In BN/BZ (1:1), on the other hand, the second-order plots are slightly bent, suggesting that ion radicals are not always freely solvated; the back electron transfer may occur within a solvent-separated ion

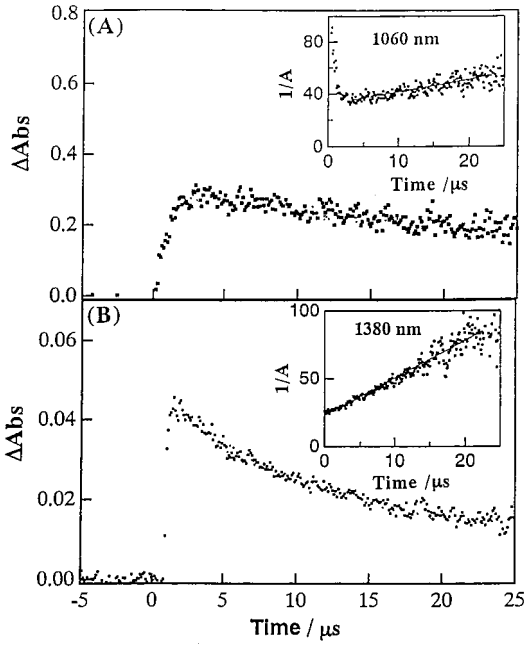

Figure 6. Decay profiles over long time scale of (A) $C_{60}^{\bullet-}$ and (B) $C_{70}^{\bullet-}$ in benzonitrile. Insert shows second-order plot. Concentrations are the same as in Figures 2 and 3.

TABLE 2: Rate Constants for Back Electron Transfer

fullerene/ amine	solvent	k_{bet}/ϵ_A[a] cm s^{-1}	k_{bet} M^{-1} s^{-1}	k_{diff} M^{-1} s^{-1}
C_{60}/PNA	BN	4.6×10^5	5.5×10^9	5.6×10^9
C_{60}/BNA	BN	5.4×10^5	6.5×10^9	5.6×10^9
C_{60}/BNA	BN/BZ	1.5×10^6	1.8×10^{10}	7.2×10^9
C_{70}/PNA	BN	1.9×10^6	7.6×10^9	5.6×10^9
C_{70}/BNA	BN	2.8×10^6	1.1×10^{10}	5.6×10^9
C_{70}/BNA	BN/BZ	4.8×10^6	1.9×10^{10}	7.2×10^9

[a] $\epsilon_A = 12000$ M^{-1} cm^{-1} at 1060 nm for $C_{60}^{\bullet-}$,[18,19] and $\epsilon_A = 4000$ M^{-1} cm^{-1} at 1380 nm for $C_{70}^{\bullet-}$.[15-18]

pair in BN/BZ (1:1). Thus, the k_{bet} values evaluated as average values are larger than the k_{diff} values.

Steady-State Photolysis and CD Spectra. Steady-state photolysis of both C_{60} and BNA with $\lambda > 330$ nm in deaerated benzonitrile solution containing C_{60} (0.2 mM) and an excess of BNA (6 mM) gave optically active adducts. As shown in the steady-state UV/vis spectra (Figure 7A), the excitation of both C_{60} and BNA in deaerated benzonitrile solution results in an increase of the absorbance at 434 nm, which is characteristic of the monoadduct,[34] suggesting C_{60}/BNA adduct formation. Figure 7B presents the CD spectra after 90 min irradiation of a deaerated benzonitrile solution of C_{60} and BNA. For *R*-(+)-BNA, a sharp positive CD band appeared at 434 nm with two broad negative CD bands at 550 and 600 nm in addition to the sharp positive CD of unreacted BNA at 380 nm. For *S*-(−)-BNA, CD bands with completely opposite sign were observed. The CD spectra in the visible region were attributed to the C_{60}/BNA adducts. These CD spectra observed in this study are characteristic of the monoadducts of fullerenes.[35] These CD spectra also show that during the photochemical reactions, no racemization of optically active BNA occurs. In contrast, no photochemical reaction could be detected upon irradiation of a mixture of C_{60} and BNA at $\lambda > 400$ nm, where the light-absorbing species is C_{60} only.

In deaerated benzene, no photochemical reaction of C_{60} with BNA occurred even by irradiation with light longer than 330 nm. As for C_{70}, no CD band appeared in the visible region both

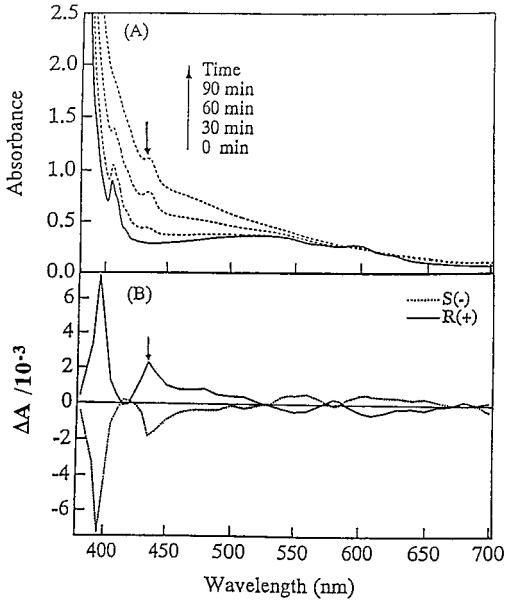

Figure 7. (A) Steady-state photolysis in the UV/vis region of deaerated benzonitrile solution containing C_{60} (0.2 mM) and *R*-(+)-BNA (6 mM) with light of $\lambda > 330$ nm. (B) CD spectra of deaerated benzonitrile solution containing C_{60} (0.2 mM) with *S*-(−)-BNA and *R*-(+)-BNA (6 mM) after irradiation with $\lambda > 330$ nm for 90 min.

in deaerated benzonitrile and in benzene by irradiation with light longer than 330 nm. In the case of C_{60}/BNA in benzonitrile, the fact that the photochemical reactions did not take place upon irradiation at wavelengths longer than 400 nm where only photoinduced electron transfer takes place yielding $C_{60}^{\bullet-}$ and $BNA^{\bullet+}$ via $^3C_{60}$* (as shown in Figure 2) indicates that the coupling reaction between $C_{60}^{\bullet-}$ and $BNA^{\bullet+}$ is less efficient than the back electron transfer.

Transient absorption spectra of BNA in deaerated benzene show the appearance of the absorption band at 480 nm corresponding to the triplet state of BNA (^{3}BNA*). This T−T absorption band was assigned by its quick decay on addition of O_2 to solution (Figure 8A). In benzonitrile, however, additional transient absorption band appeared at 520 nm, which was attributed to $BNA^{\bullet+}$ (Figure 8B) by comparison with the absorption spectrum obtained by γ-radiolysis of BNA in butyl chloride (Figure 8C).

By the steady-light photolysis of BNA in deaerated benzonitrile with light greater than 330 nm, both UV and CD spectra change as shown in Figure 9. In deaerated benzene, on the other hand, no spectral change was observed. Thus, the photochemical reactions of BNA in benzonitrile occurs via $BNA^{\bullet+}$.

Under the same experimental conditions that gave CD spectra, the transient absorption spectra were measured in the vis/NIR regions as shown in Figure 10 (355 nm excitation in benzonitrile). In addition to the transients of $^3C_{60}$* at 740 nm and $C_{60}^{\bullet-}$ at 1060 nm, the transient band of $BNA^{\bullet+}$ at 520 nm was also observed in the visible region. Although this spectral change is similar to the transient spectra on the basis of excitation at 532 nm (Figure 2), the main difference is that $BNA^{\bullet+}$ produced by direct excitation of BNA by 335 nm laser light is at higher concentration than that produced by 532 nm light. This is clear by comparing the intensity of the $BNA^{\bullet+}$ absorption band relative to that of $^3C_{60}$* in each case.

These findings indicate the importance of $BNA^{\bullet+}$ for formation of the adduct between C_{60} and BNA; furthermore, it is also necessary that the concentration of $BNA^{\bullet+}$ should be greater than that of $C_{60}^{\bullet-}$ for formation of the adduct between C_{60} and

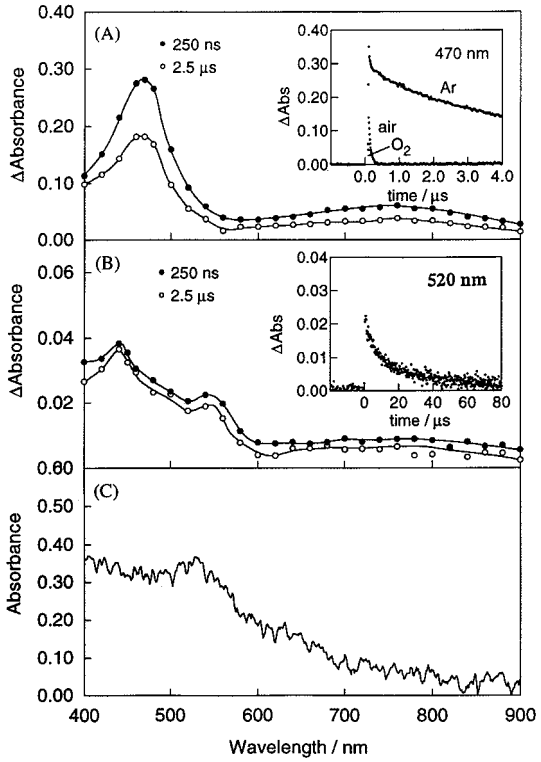

Figure 8. (A) Transient absorption spectra observed after laser photolysis of BNA (0.2 mM) with 355 nm light in Ar-saturated benzene. Insert shows time profiles of absorption bands in Ar-saturated benzene, air, and oxygen. (B) Transient absorption spectra observed after laser photolysis of BNA (0.1 mM) in Ar-saturated benzonitrile with 355 nm light after 0.25 and 2.5 μs. Insert shows time profile. (C) Steady-state spectrum obtained by γ-radiolysis of BNA in butyl chloride glass at 77 K.

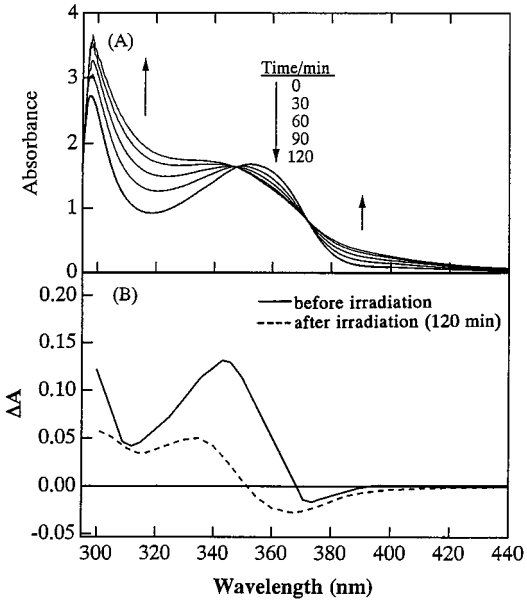

Figure 9. Steady-state photolysis of *R*-(+)-BNA (0.2 mM) with light of λ > 330 nm in Ar-saturated benzonitrile: (A) UV spectra and (B) CD spectra.

BNA. Although $BNA^{\bullet+}$ produced by electron transfer via $^3C_{60}$* may return to BNA by back electron transfer with equimolar $C_{60}^{\bullet-}$, excess $BNA^{\bullet+}$ produced by direct photoejection may remain after back electron transfer and dissociate into H^+ and the N-centered radical, which then adds to C_{60}. The deprotonation process (k_d) may be slower than back electron transfer.

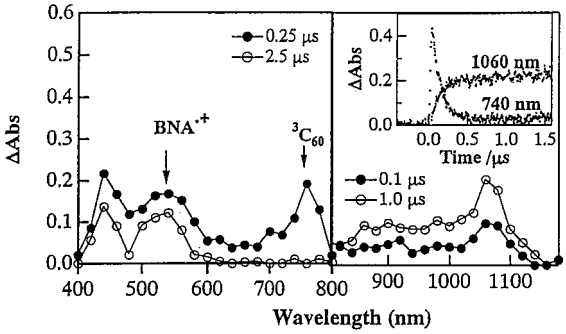

Figure 10. Transient absorption spectra obtained after 355 nm laser pulsing in deaerated benzonitrile solution of C_{60} (0.1 mM) and BNA (3 mM) in the vis/NIR regions. Insert shows time profiles.

SCHEME 1: Excitation (λ > 330 nm) in Ar-Saturated BN Solution

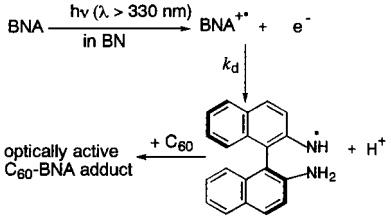

The reaction mechanism presumed in this study is illustrated in Scheme 1. The structure analysis of the adduct by NMR or mass spectra was complicated because benzonitrile could not be completely removed even after prolonged drying at high vacuum (at room temperature), in addition to the instability of the adduct.[36]

Conclusions

The efficiency of photoinduced electron transfer from BNA or PNA to the excited triplet states of fullerenes depends on the molecular structure of the electron donor, as shown in differences in the Φ_{et}^T values. This reflects the role of hindrance of approach of BNA with its perpendicular π-system to round fullerenes. This study also demonstrates the formation of optically active adducts upon irradiation of a mixture of C_{60} and BNA at λ > 330 nm in deaerated benzonitrile by CD measurement, which is useful for detecting unstable optically active adducts of fullerenes. By combining laser flash photolysis with CD measurement, we revealed that the higher concentration of $BNA^{\bullet+}$ compared with that of $C_{60}^{\bullet-}$ is indispensable to produce the optically active adduct between C_{60} and BNA.

Acknowledgment. The present work was partly supported by the Grant-in-Aid on Priority-Area-Research on "Laser Chemistry of Single Nanometer Organic Particle" (No. 10207202) and on "Carbon Alloys" (No. 10137203) from the Ministry of Education, Science, Sports and Culture of Japan. M. El-Kemary also thanks the Ministry of High Education and Scientific Research of Egypt and Mr. M. M. Alam for his technical help.

References and Notes

(1) Sension, R.; Szarka, A. Z.; Smith, G. R.; Hochstrasser, R. M. *Chem. Phys. Lett.* **1991**, *185*, 179.

(2) Arbogast, J. W.; Foote, C. S. *J. Am. Chem. Soc.* **1991**, *113*, 8886.

(3) Biczok, L.; Linschitz, H. *Chem. Phys. Lett.* **1992**, *195*, 339.

(4) Nonell, S.; Arbogast, J. W.; Foote, C. S. *J. Phys. Chem.* **1992**, *96*, 4169.

(5) Guldi, D. M.; Hungerbuhler, H.; Janata, E.; Asmus, K.-D. *J. Chem. Soc., Chem. Commun.* **1993**, 84.

(6) Ghosh, H.; Pal, H.; Sapre, A. V.; Mittal, J. P. *J. Am. Chem. Soc*. **1993**, *115*, 11722.

(7) Osaki, T.; Tai, Y.; Tazawa, M.; Tanemura, S.; Inukawa, K.; Ishiguro, K.; Sawaki, Y.; Saito, Y.; Shinohara, H.; Nagashima, H. *Chem. Lett.* **1993**, 789.

(8) Ito, O.; Sasaki, Y.; Yoshikawa, Y.; Watanabe, A. *J. Phys. Chem*. **1995**, *99*, 9838.

(9) (a) Ettl, R.; Chao, I.; Diederich, F.; Whetten, R. L. *Nature* **1991**, *353*, 149. (b) Herrmann, A.; Diederich, F. *Helv. Chim. Acta* **1996**, *79*, 1741.

(10) (a) Hawkins, J. M.; Meyer, A.; Nambu, M. *J. Am. Chem. Soc*. **1993**, *115*, 9844. (b) Hawkins, J. M.; Nambu, M.; Meyer, A. *J. Am. Chem. Soc*. **1994**, *116*, 7642.

(11) (a) Vasella, A.; Uhlmann, P.; Waldraff, C. A.; Diederich, F.; Thilgen, C. *Angew. Chem., Int. Ed. Engl.* **1992**, *31*, 1388. (b) Nierengarten, J.-N.: Habicher, T.; Kessinger, R.; Cardullo, F.; Diederich, F. *Helv. Chim. Acta* **1997**, *80*, 2238.

(12) (a) Wilson, S. R.; Wu, Y.; Kaprinidis, N. A.; Schuster, D. I.; Welch, C. J. *J. Org. Chem.* **1993**, *58*, 6548. (b) Wilson, S. R.; Lu, Q.; Cao, J.; Wu, Y.; Welch, C. J.; Schuster, D. I. *Tetrahedron* **1996**, *52*, 5131.

(13) (a) Gross, B.; Churig, V.; Lamparth, I.; Herzog, A.; Djojo, F.; Hirsh, A. *J. Chem. Soc., Chem. Commun.* **1967**, 1117. (b) Schick, G.; Hirsch, A. *Tetrahedron* **1998**, *54*, 4283.

(14) (a) Prato, M.; Bianco, A.; Maggini, M.; Scorrano, G.; Toniolo, C.; Wudl, F. *J. Org. Chem.* **1993**, *58*, 5578. (b) Bianco, A.; Maggini, M.; Scorrano, G.; Toniolo, C.; Marconi, G.; Villani, C.; Prato, M. *J. Am. Chem. Soc*. **1996**, *118*, 4072.

(15) (a) Alam, M. M.; Watanabe, A.; Ito, O. *J. Org. Chem.* **1995**, *60*, 3440. (b) Watanabe, A.; Ito, O. *J. Phys. Chem*. **1994**, *98*, 7736.

(16) (a) Sension, R. J.; Szarka, A. Z.; Smith, G. R.; Hochstrasser, R. M. *Chem. Phys. Lett.* **1991**, *185*, 179. (b) Arbogast, J. W.; Foote, C. S.; Kao, M. *J. Am. Chem. Soc.* **1992**, *114*, 2277. (c) Nonell, S.; Arbogast, J. W.; Foote, C. S. *J. Phys. Chem.* **1992**, *96*, 4169.

(17) (a) Sasaki, Y.; Fujitsuka, M.; Watanabe, A.; Ito, O. *J. Chem. Soc., Faraday Trans*. **1997**, *93*, 4275. (b) Nojiri, T.; Alam, M. M.; Konami, H.; Watanabe, A.; Ito, O. *J. Phys. Chem. A* **1997**, *101*, 7943.

(18) Kato, T.; Kodama, T.; Shida, T.; Nakagawa, T.; Matsui, Y.; Suzuki, S.; Shiromaru, H.; Yamauchi, K.; Aciba, Y. *Chem. Phys. Lett*. **1991**, *180*, 446.

(19) Greaney, M. A.; Gorun, S. M. *J. Phys. Chem*. **1991**, *96*, 7142.

(20) Gasyna, Z.; Andrews, L.; Schatz, P. N. *J. Phys. Chem.* **1992**, *96*, 1525.

(21) Guldi, D. M.; Hungerbuhler, H.; Janata, E.; Asmus, K.-D. *J. Phys. Chem.* **1993**, *97*, 11258.

(22) Arbogast, J. W.; Diederich, F. N.; Alvarez, M. M.; Anz, S. J.; Whetten, R. L. *J. Phys. Chem.* **1991**, *95*, 11.

(23) Heath, G. A.; McGrady, J. E.; Martin, R. L. *J. Chem. Soc., Chem. Commun.* **1992**, 1272.

(24) Wasielewski, M. R.; O'Neil, M. P.; Lykke, K. R.; Pellin, M. J.; Gruen, D. M. *J. Am. Chem. Soc*. **1991**, *113*, 2774.

(25) Tanigaki, K.; Ebbesen, T. W.; Kuroshima, S. *Chem. Phys. Lett.* **1991**, *185*, 189.

(26) Dimirijevic, N. M.; Kamat, P. V. *J. Phys. Chem.* **1992**, *96*, 4811.

(27) Etheridge, H. T.; Weisman, R. B. *J. Phys. Chem.* **1995**, *99*, 27822.

(28) Lawson, D. R.; Feldhein, D. L.; Foss, C. A.; Dorhout, P. K.; Elliott, C. M.; Martin, C. R.; Parkinson, B. *J. Phys. Chem.* **1992**, *96*, 7175.

(29) Gorun, S.; Greaney, M.; Day, V.; Day, C.; Upton, R.; Briant, C. In *Fullerenes*; Hammond, G. Kuck, V., Eds.; ACS Symposium Series 481; American Chemical Society: Washington, DC, 1992; p 41−53.

(30) Hase, H.; Hiyataka, Y. *Chem. Phys. Lett.* **1993**, *215*, 141.

(31) Nakamura, H.; Tanaka, J.; Nakashima, N.; Yoshihara, K. *Bull. Chem. Soc. Jpn.* **1982**, *55*, 1795.

(32) Stere, C. A.; Von Willigen, H.; Biczok, K.; Gupta, N.; Linschitz, H. *J. Phys. Chem.* **1996**, *100*, 8920.

(33) Guldi, D. M.; Asmus, K.-D. *J. Am. Chem. Soc.* **1997**, *119*, 5744.

(34) Mikami, K.; Matsumoto, S.; Ishida, A.; Takamuku, S.; Suenobu, T.; Fukuzumi, S. *J. Am. Chem. Soc*. **1995**, *117*, 11134.

(35) Herman, A.; Diederich, F. *Helv. Chem. Acta* **1996**, *79*, 1741.

(36) Skieb, A.; Hirsh, A. *J. Chem. Soc., Chem. Commun.* **1994**, 355.